

# Scale-factor-stabilized fiber-optic gyroscope by deep phase modulation

Pie-Yau Chien and Ci-Ling Pan

*Institute of Electro-Optical Engineering, National Chiao-Tung University, Hsinchu, Taiwan 30050, China*

Received October 10, 1991

A scale-factor-stabilized fiber-optic gyroscope by deep phase modulation is demonstrated. There are two servo loops included in this system. The first servo loop is used for stabilization of the light intensity output of the fiber-optic gyroscope. The second loop is used to stabilize the phase-modulation index. The third-harmonic frequency of the phase-modulation signal is used for detection of the Sagnac phase shift by the lock-in technique.

Many proposed signal-processing techniques have been implemented in detecting the Sagnac phase shift of the fiber-optic gyroscope<sup>1-14</sup> (FOG). One of the simplest signal detection methods utilizes the dynamic phase bias followed by the lock-in technique.<sup>1-6</sup> In order to enhance the linearity and dynamic range of the FOG, two novel techniques have also been demonstrated successfully. The first is the pseudoheterodyne (phase-reading) method, in which the optical phase shift is downconverted to an electrical signal at low frequency. The Sagnac phase shift is then measured by a phase meter at the electrical frequency.<sup>7-9</sup> The second technique is signal processing in the closed-loop configuration, which is implemented by using the acousto-optic frequency shifter,<sup>10</sup> the sawtooth phase modulation signal,<sup>11,12</sup> or the gated phase-modulation signal.<sup>13,14</sup> For a highly accurate open-loop FOG, the lock-in technique is still the most sensitive technique for signal detection at present. In order to stabilize the scale factor of such a FOG, an additional servo loop that is included in the lock-in detection technique has also been developed successfully for this purpose, e.g., the dividing method,<sup>2</sup> the peak detection method,<sup>4</sup> and the double lock-in method.<sup>5</sup> These methods have all been applied to stabilize the light intensity output of the FOG. For the modulation index stabilization, the dividing method<sup>2</sup> for  $J_2(\phi_e)/J_4(\phi_e)$  and the amplitude switching method<sup>6</sup> have also been demonstrated. In this Letter I propose and demonstrate a novel method for stabilization of the light intensity output, the polarization fluctuation, and the phase-modulation index of the FOG simultaneously. The basic ideas of this approach are (i) the application of a deep phase-modulation index to the FOG, followed by gated switching of the signal to detect the fluctuation in the light intensity output, and (ii) the use of the third-harmonic frequency component of the phase-modulation signal for stabilization of the modulation index at  $J_3(\phi_e)|_{\max}$ .

The basic operating principle of this method is as follows: A deep sinusoidal signal  $\phi_m \cos \omega_m t$  as shown in Fig. 1(a) is employed as the phase-

modulation signal. The detected signal,  $V_{\text{out}}(t)$ , at an ac-coupling amplifier of an open-loop FOG can be written as

$$V_{\text{out}}(t) = GP_0\gamma \cos(\phi_e \cos \omega_m t - \Delta\phi_R), \quad (1)$$

where  $G$  is the conversion gain of the optical receiver,  $P_0$  is the output power of the light source,  $\gamma$  is the polarization-state-induced signal fading,  $\phi_e = 2\phi_m \sin \omega\tau/2$  is the effective phase-modulation index, and  $\tau$  is the time delay of the fiber loop. Under the condition of  $\phi_e > \pi$ , the sinusoidal waveform of the phase-modulation signal can be approximated by a triangular waveform within some effective period to scan the interferometric signal. Thus the output signal of the FOG can be divided into two different output forms by the time-gating technique. For  $P_0\gamma$  stabilization, a gate-switching signal is used to select the effectively linearly phase-modulated re-

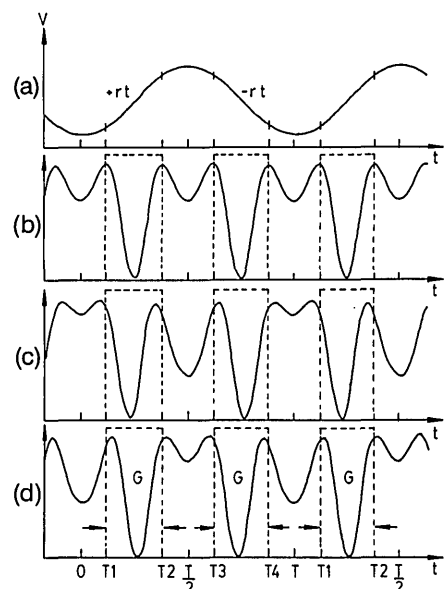


Fig. 1. Operation principle for detection of the variation in the amplitude of  $P_0\gamma$ . (a) The applied phase-modulation signal, where  $\phi_e \cong 4.2$  rad and  $J_3(\phi_e)$  is maximum. (b)-(d) The output signals of the FOG under different Sagnac phase bias.

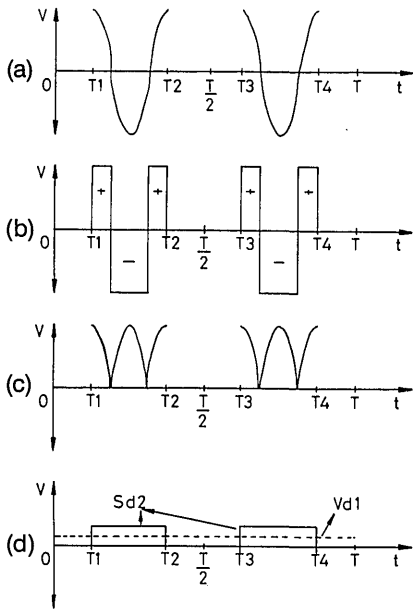


Fig. 2. Signal processing in the  $P_0\gamma$  detection. (a) The gated output signal  $V_{out,G}(t)$  in phase bias  $\Delta\phi_R = 0$ , (b) the generated switching signal  $S(t)$  from  $V_{out,G}(t)$ , (c) the signal after the switching-type mixer, (d) the signal after the low-pass filter.

gion. The output signal after the gate switching can be expressed as

$$V_{out,G}(t) = \begin{cases} GP_0\gamma \cos(\omega_{eff}t + \Delta\phi_R) & T_1 < t < T_2, \\ GP_0\gamma \cos(\omega_{eff}t - \Delta\phi_R) & T_3 < t < T_4, \\ 0 & 0 < t < T_1, T_2 < t < T_3, T_4 < t < T, \end{cases} \quad (2)$$

where  $\omega_{eff}$  is the effective angular frequency of the beat signal generated by the linearly scanned effective triangular waveform and  $|T_2 - T_1|$  and  $|T_4 - T_3|$  are the pulse widths of the gate-switching signal within the positive and negative slope of the effective triangular waveform. The output signal of the FOG before the gate switching is shown in Figs. 1(b)–1(d) for a different Sagnac phase shift  $\Delta\phi_R$ . It is shown that within the gating time intervals,  $|T_2 - T_1|$  and  $|T_4 - T_3|$ , a beat signal is observed, and the Sagnac phase shift is included in the phase of the beat signal. Here only the case of  $\Delta\phi_R = 0$  is considered. The output signal after gate switching,  $V_{out,G}(t)$ , is shown in Fig. 2(a), which corresponds to the situation of Fig. 1(b) ( $\Delta\phi_R = 0$ ). Let the signal of  $V_{out,G}(t)$  go through a zero-crossing circuit; then a switching signal  $S(t)$  as shown in Fig. 2(b) is generated that can be expressed as

$$S(t) = \begin{cases} +1 & \text{within a positive-polarity region} \\ -1 & \text{within a negative-polarity region.} \end{cases} \quad (3)$$

The signals  $S(t)$  and  $V_{out,G}(t)$  are then mixed by a double-balance switching-type mixer. The output signal at the mixer is shown in Fig. 2(c). Its operating principle can be considered as that of a lock-in amplifier without a time delay between the reference signal and the input signal. This mixed output signal is then sent through a low-pass filter, and the output signal of the low-pass filter is shown in Fig. 2(d), where  $S_{d2}(t)$  is the dc term of the  $V_{out,G}(t)$

within the gate-switching region and  $V_{d1}(t)$  is the average dc term within the full period of  $T$ . The magnitude of  $V_{d1}(t)$  can be written as

$$V_{d1}(t) = KGP_0\gamma(2/T)T_{eff}, \quad (4)$$

where  $K$  is the conversion gain of the mixer,  $T_{eff} \equiv |T_2 - T_1| = |T_4 - T_3|$ , and  $T$  is the period of the phase-modulation signal. From Eq. (4) it can be seen that the drift in  $P_0$  and  $\gamma$  can be detected independently of the Sagnac phase shift. There is a criterion for an optimum choice of the pulse widths  $T_2 - T_1$  and  $T_4 - T_3$ —the duty cycle needs to be adjusted such that the nonlinear region of the sinusoidal signal is eliminated. For this experiment the duty cycle of the gate switching in our system is selected to be less than 70% of the half-period  $T/2$  of the modulation signal. It is easy to check the output signal of the FOG by rotating the gyroscope such that the information on the rotation rate is included in the phase of the angular frequency  $\omega_{eff}$  only.

The second output signal form is obtained by expanding Eq. (1) by using the Bessel function and demodulating it with a lock-in amplifier at the reference frequency of  $3f_m$ . Thus we can obtain

$$V_{lock-in,I}(t) = GP_0\gamma J_3(\phi_e) \sin \Delta\phi_R, \quad (5)$$

where the gain of the lock-in amplifier is included in

the factor  $G$ . We assume that the term  $P_0\gamma$  has been stabilized with the output of the mixer based on Eq. (4). The scale factor that remains to be stabilized is the term  $J_3(\phi_e)$ , or  $\phi_e$ . This can be realized by controlling  $J_3(\phi_e)$  such that it is sustained at the maximum value for the highest sensitivity by using an amplitude-modulated phase-modulation signal followed by a lock-in demodulation circuit. The

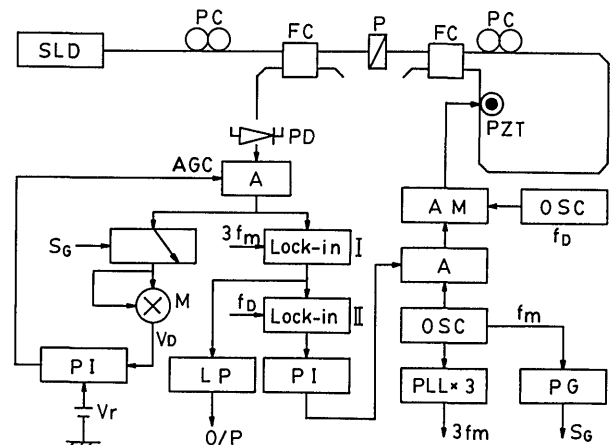


Fig. 3. Block diagram of experimental setup. FC, fiber coupler; P, polarizer; PD, photodetector; A, amplifier; AGC, automatic gain control; M, multiplier;  $S_G$ , gate-switching signal; PG, pulse gate-switching signal generator; OSC, sinusoidal signal generator; PLL  $\times$  3, phase-locked loop  $3f_m$  reference signal generator.

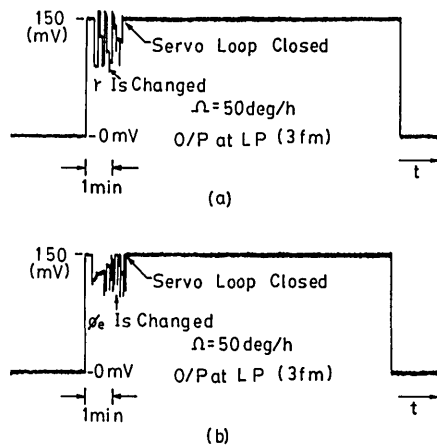


Fig. 4. Free-running and closed-loop values of the FOG output, after the low-pass filter at the lock-in amplifier I output, for a fixed rotation rate of 50 deg/h. (a) The polarization-state-induced signal fading  $\gamma$  was changed, (b) the phase-modulation index  $\phi_e$  was changed.

condition that  $J_3(\phi_e)$  is at its maximum corresponds to the case when  $\phi_e \cong 4.2$ . This implies that the requirement of deep phase modulation,  $\phi_e > \pi$ , is satisfied. Under this condition the demodulation of  $P_0\gamma$  also works well.

The experimental setup of the FOG is shown in Fig. 3. The gyroscope was formed by using single-mode fiber coils 12 cm in diameter. The relation between the Sagnac phase shift and the rotation rate was  $\Delta\phi_R$  (deg) =  $2.0 \Omega$  (deg/s). A superluminescent laser diode (SLD) was used as the light source to reduce noise. An in-line piezoelectric transducer (PZT) was used as the phase modulator, and its modulation frequency was 40.0 kHz. The amplitude of the phase-modulation signal was adjusted such that  $J_3(\phi_e)$  is at its maximum. The output signal after the preamplifier followed two paths. One path is used for the stabilization of the  $P_0\gamma$  term, while the other path is used for  $\phi_e$  stabilization. For the  $P_0\gamma$  stabilization path, a gate-switching signal synchronized to the phase-modulation signal with a pulse width from  $|T_1 - T_2| = |T_4 - T_3| \cong 0.7(T/2)$  to  $0.2(T/2)$  was suitable for  $P_0\gamma$  detection. In this experiment the  $0.7(T/2)$  value was used for maximum sensitivity. By comparing it with a stable reference voltage  $V_r$ , we can stabilize  $P_0\gamma$  by controlling the gain of the preamplifier. For stabilization of the phase-modulation index  $\phi_e$ , a reference frequency of  $3f_m$  was generated from the phase-modulation signal of  $f_m$ . The  $3f_m$  signal was used to detect the variation in  $J_3(\phi_e)$  and also the output of the FOG by using lock-in amplifier I (lock-in I). A small modulation signal at  $f_D = 1.0$  kHz was used to modulate the amplitude (AM) of the phase-modulation signal so that the modulation index shift from  $J_3(\phi_e)|_{\max}$  could be detected. The output signal of lock-in I was then sent to lock-in II. The deviation of  $J_3(\phi_e)$  from its maximum value can thus be

demodulated by using another lock-in amplifier (lock-in II) at the reference frequency  $f_D$ . The output signal from lock-in II was sent through proportional and integrating (PI) compensating circuits so that the amplitude of the phase-modulation signal could be controlled. The loop gain of the  $\phi_e$  stabilization loop was influenced by the Sagnac phase shift  $\Delta\phi_R$ ; however, it can be eliminated by the PI compensating circuit. Thus the phase-modulation index  $\phi_e$  was stabilized such that the value of  $J_3(\phi_e)$  was at a maximum.

In order to examine the stability of the scale factor of the FOG, two polarization controllers (PC's) and an adjustable attenuator for the phase-modulation signal were used to generate the variations in  $\gamma$  and  $\phi_e$ . Figure 4(a) shows the output signal at the output of the low-pass filter (LP) after lock-in I under free-running and closed-loop conditions when  $\gamma$  was varied. Figure 4(b) shows the output signal when  $\phi_e$  was varied. This figure shows that the stabilization loop was worked well. Since the output signal of the FOG at the lock-in amplifier is  $V_{\text{out}}(t) = P_0\gamma J_3(\phi_e)\sin\phi_R$ , a rotation bias of  $\phi_R$  must be included so that the stability of  $P_0\gamma J_3(\phi_e)$  can be examined. In these experiments a rotation bias rate of 50 deg/h was present, and the bandwidth of the measurement system was 10 Hz. From Figs. 4(a) and 4(b) it is calculated that a scale-factor stability of the FOG of  $\Delta S/S \leq 1.0 \times 10^{-4}$ , where the scale factor is defined as  $S \equiv P_0\gamma J_3(\phi_e)$ , was achieved.

In summary, a novel method that uses the deep phase-modulation method to stabilize the scale factor of an open-loop FOG has been demonstrated. In this method the time-gating and lock-in techniques are combined to detect different components of the scale factor and stabilize them separately.

## References

1. R. A. Bergh, H. C. Lefevre, and H. J. Shaw, *Opt. Lett.* **6**, 502 (1981).
2. K. Bohm, P. Marten, K. Petermann, and E. Weidel, *Electron. Lett.* **19**, 997 (1983).
3. E. Kiesel, *Proc. Soc. Photo-Opt. Instrum. Eng.* **838**, 129 (1987).
4. R. P. Moeller, W. K. Burns, and N. J. Frigo, *IEEE J. Lightwave Technol.* **7**, 262 (1989).
5. P.-Y. Chien and C.-L. Pan, *Opt. Lett.* **16**, 426 (1991).
6. N. J. Frigo, in *Digest of Conference on Optical Fiber Sensors* (Optical Society of America, Washington, D.C., 1986), p. 181.
7. A. D. Kersey, A. C. Lewin, and D. A. Jackson, *Electron. Lett.* **20**, 368 (1984).
8. B. Y. Kim and H. J. Shaw, *Opt. Lett.* **9**, 378 (1984).
9. M. Oh and Y. Kim, *Opt. Lett.* **13**, 521 (1988).
10. J. L. Davis and S. Ezekiel, *Opt. Lett.* **6**, 505 (1981).
11. A. Ebbergh and G. Schiffner, *Opt. Lett.* **10**, 300 (1985).
12. C. J. Kay, *IEE Proc.* **132**, 259 (1985).
13. B. Y. Kim and H. J. Shaw, *Opt. Lett.* **9**, 263 (1984).
14. B. Y. Kim and H. J. Shaw, *Opt. Lett.* **9**, 375 (1984).